Available online at www.sciencedirect.com

SciVerse ScienceDirect

Ceramics International 38 (2012) 2333–2338

CERAMICS INTERNATIONAL

www.elsevier.com/locate/ceramint

Preparation of new heteronuclear $(NH_4)RE[Fe^{II}(CN)_6]\cdot nH_2O$ complexes (RE = La, Ce, Pr, Nd, Sm, Gd, Dy, Y, Er, Lu) and their low-temperature decomposition for perovskite-type oxide

Hiromichi Aono [a,*], Takaaki Nishida [a], Masato Kurihara [b], Masatomi Sakamoto [b], Yoshihiko Sadaoka [a]

[a] *Materials Science and Biotechnology, Graduate School of Science and Engineering, Ehime University, 3 Bunkyo-cho, Ehime 790-8577, Japan*

[b] *Material and Biological Chemistry, Graduate School of Science and Engineering, Yamagata University, 1-4-12, Kojirakawa-machi, Yamagata 990-8560, Japan*

Received 6 October 2011; received in revised form 7 October 2011; accepted 31 October 2011

Available online 6 November 2011

Abstract

New heteronuclear $(NH_4)RE^{III}[Fe^{II}(CN)_6]\cdot nH_2O$ complexes (RE = La, Ce, Pr, Nd, Sm, Gd, Dy, Y, Er, Lu) were synthesized and their thermal decomposition products were investigated. The crystal structure of $(NH_4)RE[Fe^{II}(CN)_6]\cdot nH_2O$ would be a hexagonal unit cell (space group: $P6_3/m$), which was the same as that of $La[Fe^{III}(CN)_6]\cdot 5H_2O$. The hydration number $n = 4$ was estimated by TG results for all the RE complexes. The lattice constants depended on the ionic radius of the RE^{3+} ion for the heteronuclear complexes. The single phase of the perovskite type materials was directly obtained by decomposition of the heteronuclear complexes for RE = La, Pr, Nd, Sm, and Gd. A mixture of CeO_2 and Fe_2O_3 was formed for RE = Ce because of its oxidation to Ce^{4+}. In the case of RE = Dy, Y, Er, and Lu complexes, the perovskite type materials formed at higher temperature via. mixed oxides such as RE_2O_3 and $RE_4Fe_5O_{13}$ due to the small RE^{3+} ionic radius.

Keywords: Hetronuclear complex; $(NH_4)RE[Fe^{II}(CN)_6]\cdot nH_2O$; Thermal decomposition; Perovskite-type oxide

1. Introduction

The perovskite-type $REMO_3$ oxides having rare earth elements (RE) and trivalent transition cations (M) have been extensively studied for their practical uses as catalysts [1–7], electrode materials in fuel cells [8–10], gas sensors [11–15], oxygen permeable membranes [16] and platinum-free alkaline water electrolysis cells [17]. A solid state reaction method or chemical processing methods have been widely adopted for the preparation of such perovskite-type oxides. The solid-state reaction of RE_2O_3 and M_2O_3 single oxides is the most conventional method for the preparation of these heterometallic oxides. However, with this method, it is very difficult to control the powder quality and particle size because of its high calcination temperature (usually above 1273 K). The synthesis using chemical processing methods such as a co-precipitation method, sol–gel method, and glycothermal method is performed at considerably lower temperatures than that through solid-state reaction methods, and finer perovskite-type products are obtainable.

As another chemical method, the thermal decomposition of the appropriate heteronuclear complexes containing RE:M = 1:1 ratio from the hexacyano complexes has been investigated for the preparation of the homogeneous perovskite-type oxides having finer size particles [18]. Especially, nanoparticles of $LaFeO_3$ were found to form by the thermal decomposition of $La[Fe^{III}(CN)_6]\cdot 5H_2O$, which is a coordination polymer having a three-dimensional network structure with Fe^{III}–CN–La^{III} linkages, even at a low temperature of 623 K [19]. $REMO_3$ (RE = trivalent rare earth ions, M = Fe^{III} or Co^{III}) and related perovskite-type materials have been prepared from the corresponding cyano-bridged coordination polymer precursors, $RE[M^{III}(CN)_6]\cdot nH_2O$ based heteronuclear complexes [20–25]. As similar complexes, the thermal decomposition of $KLn[Fe^{II}(CN)_6]\cdot nH_2O$ (Ln = lanthanide) has been reported by Goubard and Tabuteau [26,27]. However, this

* Corresponding author. Tel.: +81 89 927 9856; fax: +81 89 927 9856.
E-mail address: aono.hiromichi.mf@ehime-u.ac.jp (H. Aono).

0272-8842/$36.00
doi:10.1016/j.ceramint.2011.10.085

material has a serious problem in that K^+ ions remain in the perovskite-type oxides formed. We synthesized a K-free new $(NH_4)La[Fe^{II}(CN)_6]\cdot nH_2O$ complex and briefly reported this complex and its thermal decomposition products [28].

In this study, we studied new $(NH_4)RE[Fe^{II}(CN)_6]\cdot nH_2O$ complexes (RE = La, Ce, Pr, Nd, Sm, Gd, Dy, Y, Er, Lu) and their thermal decomposition products.

2. Experimental

The complex $(NH_4)RE[Fe^{II}(CN)_6]\cdot nH_2O$, was almost quantitatively synthesized by mixing equivalent amounts of $RE(NO_3)_3\cdot nH_2O$, RE^{III} = La, Ce, Pr, Nd, Sm, Gd, Dy, Y, Er, Lu (50 mmol in 20 ml water), and $(NH_4)_4[Fe^{II}(CN)_6]\cdot nH_2O$ (ca. 14.4 wt.% H_2O content) (Wako Pure Chemical Industries, Ltd.) (50 mmol in 20 ml water) under continuous stirring. After that, 400 ml of methyl alcohol was added in the mixed solution and then stirred for 1 h at 60–70 °C. The resulting precipitate was collected by suction filtration and then washed with a small amount of water and methyl alcohol before drying in ambient air. The complexes decomposed at low temperature for 1 h to obtain the perovskite-type $REFeO_3$ powders.

The thermal decomposition process of the complex and the sintering process were studied by thermogravimetric analysis with differential thermal analysis (TG/DTA, Seiko Instrument TG/DTA 32), performed with a heating rate of 10 °C/min in dry air. The sample powder was dried at 50 °C for 2 h in dry air before the TG/DTA measurement. X-ray diffraction analysis (XRD, Model Rint 2000, Rigaku Corporation, using Cu-K_α radiation) was used to investigate the structure of the thermal decomposition products. Specific surface areas were determined by the BET method (Belsorp-mini, BEL Japan) at 77 K. The homogeneity of the samples was analyzed using SEM-EDX (Model JSM-6510LA, JEOL Corporation). Elemental analyses of H, C, and N in the precursors were carried out at the Central Elemental Analysis Laboratory, Faculty of Science, Kyushu University, Japan. The H, C, and N elemental contents of the complex were determined by measuring H_2O, CO_2, and NO_2 concentrations in the gas formed from the decomposition of the complex at elevated temperatures.

3. Results and discussion

3.1. Complexes

Fig. 1 shows the XRD results for $(NH_4)RE[Fe^{II}(CN)_6]\cdot nH_2O$ complexes. The Millar index was shown as a hexagonal structure (space group: $P6_3/m$). The peak position was shifted to a high 2θ angle with the decrease in ionic radius of the RE^{3+} ion in the complexes. Fig. 2 shows the TG/DTA curves for the $(NH_4)La[Fe^{II}(CN)_6]\cdot nH_2O$ complex. Decomposition proceeded in a few steps from 50 to 250 °C. The weight loss percentage of the small plateau range at around 260 °C was ca. 17–18%, which is in agreement with the value (16.37%) calculated by assuming the formation of anhydride from the $n = 4$ complex. Further heating caused an abrupt weight loss at 287 °C with a strong exothermal peak in DTA result due to the decomposition of

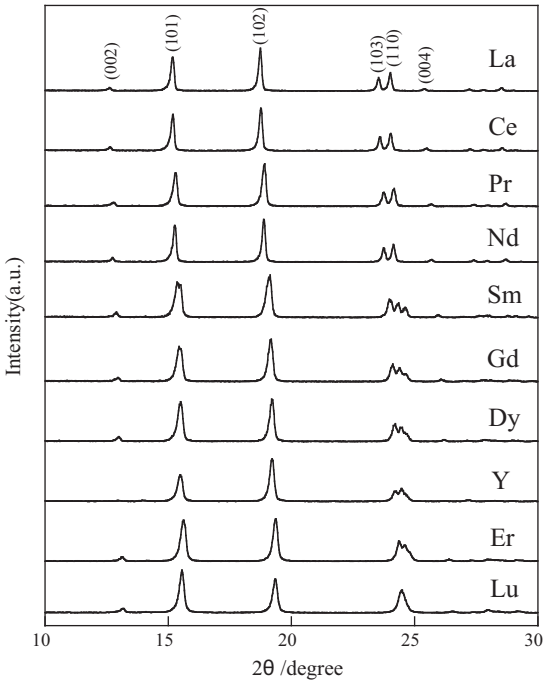

Fig. 1. XRD results of the $(NH_4)RE[Fe^{II}(CN)_6]\cdot nH_2O$ complexes (RE = La, Ce, Pr, Nd, Sm, Gd, Dy, Y, Er, Lu).

cyanide groups, and two plateaus appeared at around 300 °C and 500 °C. The final plateau was observed from 600 °C and higher temperatures. Table 1 lists the temperature of cyanide group decomposition and the final plateau, as well as the estimated n-value for the $(NH_4)RE[Fe^{II}(CN)_6]\cdot nH_2O$ complexes. The temperature of the decomposition and the final plateau tended to be comparatively small for the complexes having a large RE^{3+} ionic radius. The weight percentage 54.39 wt.% measured in the final plateau range was in good agreement with the theoretical value of 55.16 wt.%, calculated by assuming the formation of $LaFeO_3$ from the complex with 4 molecules of water tied up in the crystallization. We determined the hydration value to be $n = 4$

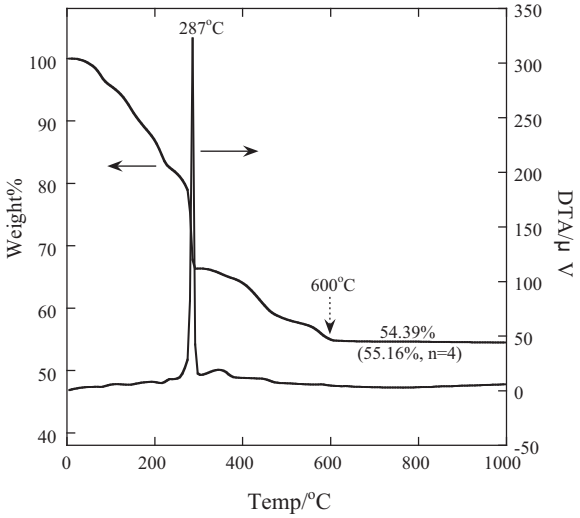

Fig. 2. TG/DTA curves of $(NH_4)La[Fe^{II}(CN)_6]\cdot nH_2O$ with the heating rate of 10 °C/min.

Table 1
TG/DTA results and estimated n value for $(NH_4)RE[Fe^{II}(CN)_6]\cdot nH_2O$ complexes (RE = La, Ce, Pr, Nd, Sm, Gd, Dy, Y, Er, Lu).

RE	CN decomp. temp. (°C)	Final plateau temp. (°C)	Final weight (%)	Theoretical weight ($n = 4$) (%)	Estimated n value
La	287	600∼	54.39	55.16	4.2
Ce	257	550∼	55.23	54.05	4.7
Pr	289	620∼	54.11	55.25	4.5
Nd	313	670∼	57.10	55.59	3.3
Sm	333	700∼	56.21	56.19	3.9
Gd	304	745∼	57.27	56.85	3.8
Dy	319	765∼	56.54	57.33	4.3
Y	316	775∼	49.37	49.30	3.9
Er	310	795∼	58.59	57.77	3.7
Lu	313	820∼	60.84	58.24	3.6

for all the complexes examined, because the estimated value using TG measurement was very close to 4 as shown in Table 1. Furthermore, the results of elemental analyses for H(2.80%), C(16.04%), and N(22.01%) were in good agreement with the theoretical values estimated to be 2.74% for H, 16.34% for C, and 22.24% for N, for the $(NH_4)La[Fe^{II}(CN)_6]\cdot nH_2O$ complex with 4 molecules of hydration water.

From the XRD and TG results, the crystal structure for the $(NH_4)RE[Fe^{II}(CN)_6]\cdot nH_2O$ complexes can be estimated to be a hexagonal structure (space group: $P6_3/m$), which is the same as that of $La[Fe^{III}(CN)_6]\cdot 5H_2O$. In this structure, the La^{3+} site was coordinated by six nitrogens and three oxygens from CN and H_2O in the complex. There are two types of water molecules for the $La[Fe^{III}(CN)_6]\cdot 5H_2O$. Three water molecules are coordinated to the La^{3+} ion and two zeolitic water molecules are held in cavities within hydrogen bonding distance of the coordinated water molecules. For a similar complex of the $KLn[Fe^{II}(CN)_6]\cdot nH_2O$ (Ln = lanthanide), three types of crystal structures have been reported as $n = 3$ (Ln = Sm, monoclinic, $P2_1/m$) [26,29], $n = 3.5$ (Ln = Gd–Lu, orthorhombic, $CmCm$) [26,27,30], and hexagonal (Ln = La–Nd, $P6_3/m$, $n = 4$) [26,31–33]. For the $n = 4$ hexagonal phase, one of the two zeolitic water molecules is replaced by a K^+ atom. For the $(NH_4)RE[Fe^{II}(CN)_6]\cdot nH_2O$ complexes, the NH_4^+ ion would exist instead of the K^+ ion (Fig. 3). Fig. 4 shows the lattice parameters for the $(NH_4)RE[Fe^{II}(CN)_6]\cdot nH_2O$ complexes. The lattice constants were linearly increased with an increase in the ionic radius (9 C.N.) of RE^{3+} ions [34]. The reported lattice parameters of $a = 0.7412$ nm and $c = 1.3943$ nm for $KLa[Fe^{II}(CN)_6]\cdot 4H_2O$ complex [32] were close with $a = 0.7417$ nm and $c = 1.403$ nm for $(NH_4)La[Fe^{II}(CN)_6]\cdot 4H_2O$ in Fig. 4, because an ionic radius of NH_4^+ is similar with that of K^+ ion. These lattice parameters would be smaller than $a = 0.7557$ nm and $c = 1.4457$ nm for the $La[Fe^{III}(CN)_6]\cdot 5H_2O$ [35] due to difference in N–O and La–O distance with the change in La–N–C angle as reported in previous study [32].

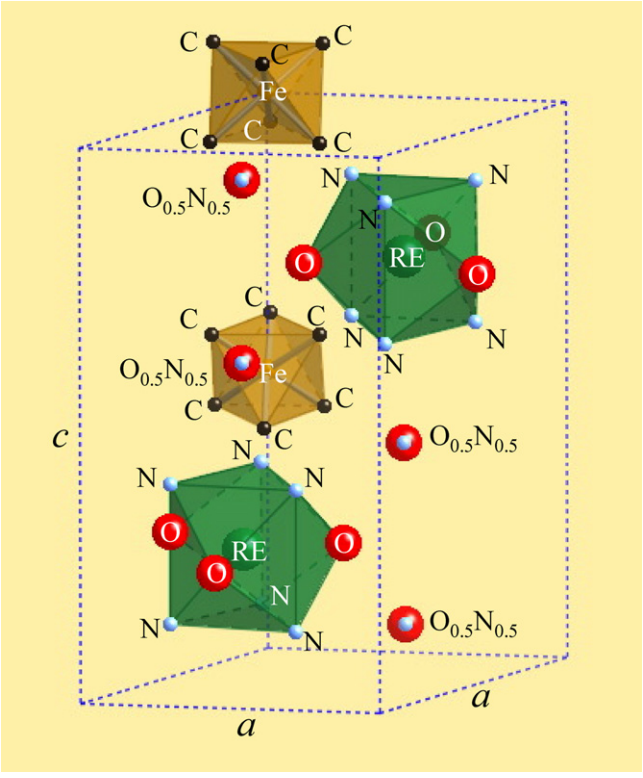

Fig. 3. Crystal structure of $(NH_4)La[Fe^{II}(CN)_6]\cdot 4H_2O$.

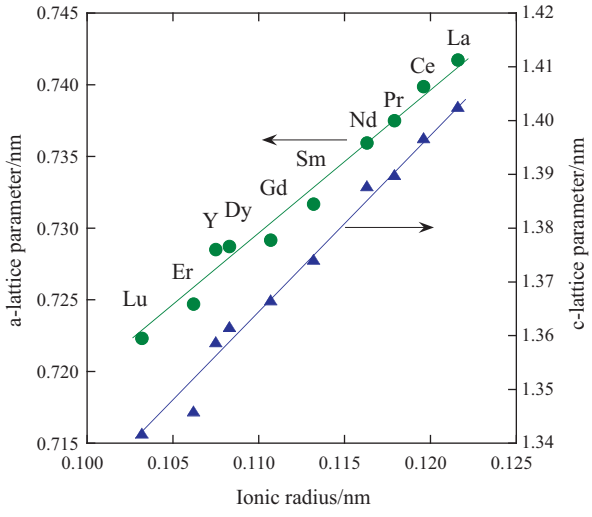

Fig. 4. The correction between the lattice parameters and ionic radius (C.N. = 9) of RE^{3+} ions for the $(NH_4)RE[Fe^{II}(CN)_6]\cdot nH_2O$ complexes and their thermal decomposition products at various temperatures.

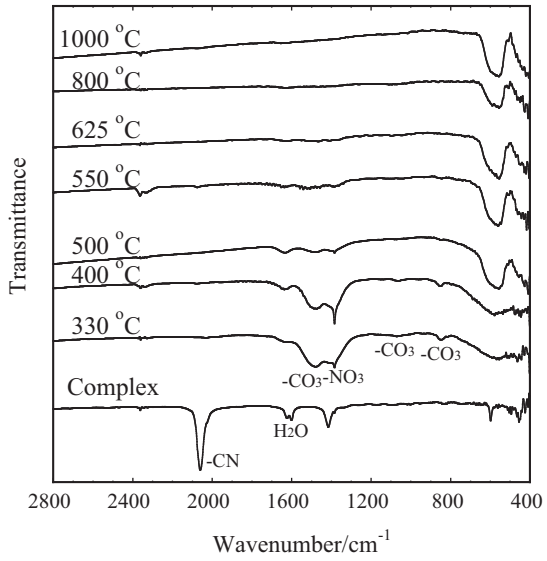

Fig. 5. FT-IR spectra of $(NH_4)La[Fe^{II}(CN)_6]\cdot nH_2O$ and its thermal decomposition products at various temperatures.

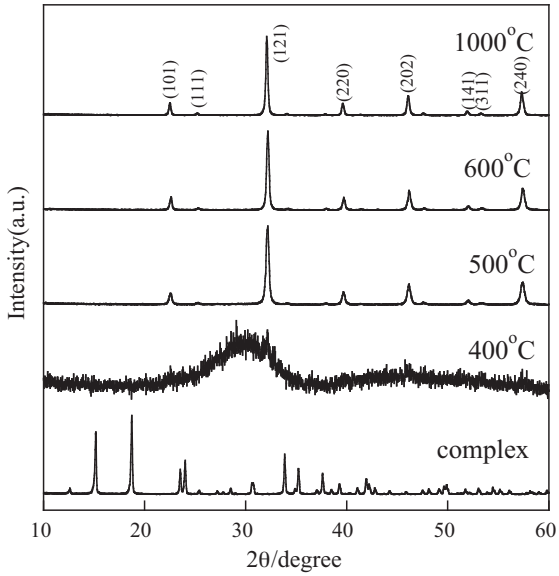

Fig. 6. XRD results of the decomposition products for $(NH_4)La[Fe^{II}(CN)_6]\cdot nH_2O$ complexes. The decomposition temperature is shown in figure.

3.2. Thermal decomposition products

Fig. 5 shows the FT-IR spectra of $(NH_4)La[Fe^{II}(CN)_6]\cdot nH_2O$ and its thermal decomposition products at various temperatures. For the as-prepared complex, a ν(CN) stretching band at about 2100 cm^{-1} and a $\delta(H_2O)$ band at about 1620 cm^{-1} were observed. The ν(CN) stretching band disappeared at 330 °C, just after the abrupt decomposition. Instead, some new bands assignable to carbonate and nitrate groups became observed around 1480, 1070 and 850 cm^{-1}, and 1385 cm^{-1}, respectively. The intensities of the absorption bands weakened for the sample calcined at 500 °C and disappeared at 625 °C and higher temperatures. This can indicated that the carbonate and nitrate groups formed by the thermal decomposition of the complex remained on the surface of the perovskite grains. This behavior agreed with the plateaus appearing at around 500 °C and the last plateau from 600 °C in the TG measurement.

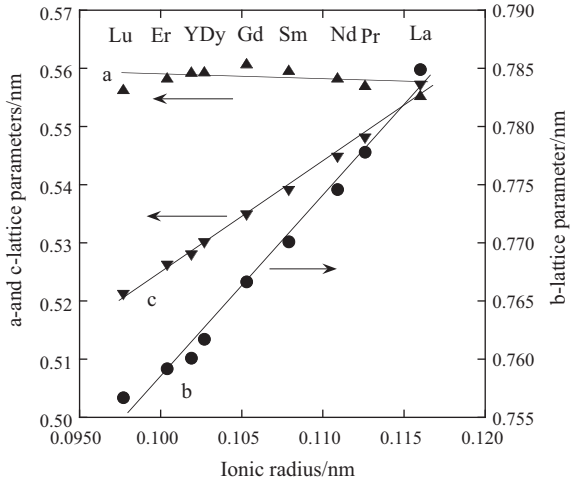

Fig. 7. The correction between the lattice parameters and ionic radius (C.N. = 8) of RE^{3+} ions for the perovskite phase obtained by the thermal decomposition of the $(NH_4)RE[Fe^{II}(CN)_6]\cdot nH_2O$ complexes at 1000 °C.

Table 2
Phase of decomposed materials at various temperatures for the $(NH_4)RE[Fe^{II}(CN)_6]\cdot nH_2O$ complexes (RE = La, Ce, Pr, Nd, Sm, Gd, Dy, Y, Er, Lu).

	La	Ce	Pr	Nd	Sm	Gd	Dy	Y	Er	Lu
1000 °C	$LaFeO_3$	CeO_2 Fe_2O_3	$PrFeO_3$	$NdFeO_3$	$SmFeO_3$	$GdFeO_3$	$DyFeO_3$	$YFeO_3$	$ErFeO_3$	$LuFeO_3$ Unknown
900 °C	$LaFeO_3$	CeO_2 Fe_2O_3	$PrFeO_3$	$NdFeO_3$	$SmFeO_3$	$GdFeO_3$	$DyFeO_3$	$YFeO_3$	$ErFeO_3$	$LuFeO_3$ Unknown
800 °C	$LaFeO_3$	CeO_2 Fe_2O_3	$PrFeO_3$	$NdFeO_3$	$SmFeO_3$	$GdFeO_3$	Dy_2O_3 $Dy_4Fe_5O_{13}$ Unknown	$YFeO_3$ Unknown	$ErFeO_3$ Unknown	$LuFeO_3$ Unknown
700 °C	$LaFeO_3$	A	$PrFeO_3$	$NdFeO_3$	$SmFeO_3$	$GdFeO_3$	A	$YFeO_3$ Unknown	$YFeO_3$ Unknown	A
600 °C	$LaFeO_3$	A	$PrFeO_3$ A	$NdFeO_3$ A	$SmFeO_3$ A	A	A	A	A	A
500 °C	$LaFeO_3$	A	$PrFeO_3$ A	A	A	A	A	A	A	A
400 °C	A	A	A	A	A	A	A	A	A	A

A, amorphous phase.

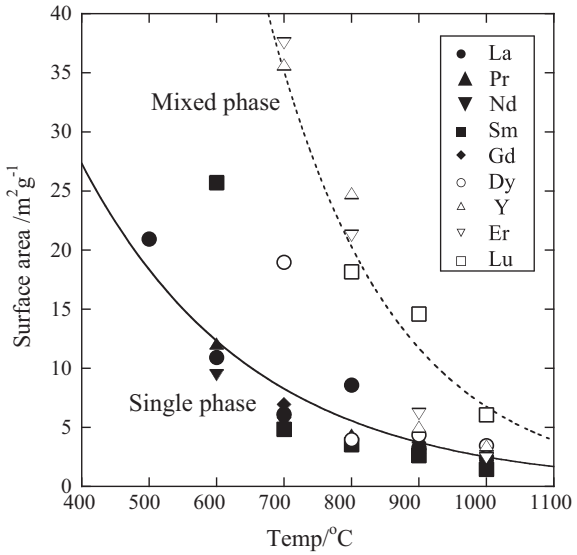

Fig. 8. Surface area results for decomposition materials at various temperatures for the $(NH_4)RE[Fe^{II}(CN)_6]\cdot nH_2O$ complexes.

The XRD profiles of the thermal decomposition products at various temperatures for $(NH_4)La[Fe^{II}(CN)_6]\cdot nH_2O$ are shown in Fig. 6. A broad band centered at about 30° as an amorphous phase was obtained for the sample calcined at 400 °C. The peaks of the $LaFeO_3$ perovskite-type phase were obtained for the samples calcined at 500 °C and the higher temperatures. The XRD profile showed only the signals due to the orthorhombic $LaFeO_3$ (space group: *Pnma*) without the broad halo patterns. It is confirmed that the full-width-at-half-maximum (FWHM) of all the $LaFeO_3$ peaks decreases with an increase in the decomposition temperature because of crystallite growth. The change in the peak position for the perovskite phase could not be confirmed with an increase in decomposition temperature from 300 °C to 1000 °C. The $LaFeO_3$ phase was directly formed from thermal decomposition of the complexes. Table 2 shows the phases of the decomposed $(NH_4)RE[Fe^{II}(CN)_6]\cdot nH_2O$ at various temperatures. For RE^{III} = La through Gd having larger ionic radius, only the peaks due to the perovskite-type oxide were observed except for Ce. In the case of RE = Ce, a mixture of CeO_2 and Fe_2O_3 was formed because of Ce^{3+} oxidation in the complex to Ce^{4+} at elevated temperature. A single phase of the perovskite-type oxide could not be directly obtained for RE = Dy through Lu having a smaller ionic radius. In this case, RE_2O_3 and RE-Fe-oxide such as $Yb_4Fe_5O_{12}$ phases were mainly formed after decomposition, and the perovskite-type phase was formed by the solid reaction at higher temperatures. Fig. 7 shows the lattice parameters as orthorhombic (*Pnma*) using the XRD results for the decomposed materials at 1000 °C. The lattice parameters for *b*- and *c*-axes increased linearly with an increase in the ionic radius of the RE^{3+} ion (C.N. = 8). On the other hand, the lattice parameter showed constant value for the *a*-axis.

Fig. 8 shows the surface area of the decomposition materials at various temperatures for the $(NH_4)RE[Fe^{II}(CN)_6]\cdot nH_2O$ complex. In the case of a single perovskite phase for RE = La through Gd, the specific surface areas of the $REFeO_3$ particles prepared in the last plateau range were ca. 20, 10, and 5 $m^2\ g^{-1}$ at 500, 600, and 700 °C, respectively. Such an increase in size and decrease in surface area are consistent with a general tendency that the particle growth proceeds as the calcination temperature is increased. For the mixed phase materials for Dy through Lu, the surface area was 2–3 times larger than those of single perovskite materials. The formation of two phases for RE_2O_3 and RE-Fe-oxide would influence the high surface area compared with that of a single $REFeO_3$ phase. Fig. 9 shows the SEM-EDX results for the $(NH_4)La[Fe^{II}(CN)_6]\cdot nH_2O$ complex and its decomposition sample at 500 °C. The samples were pressed to obtain a flat surface. Elemental analyses were

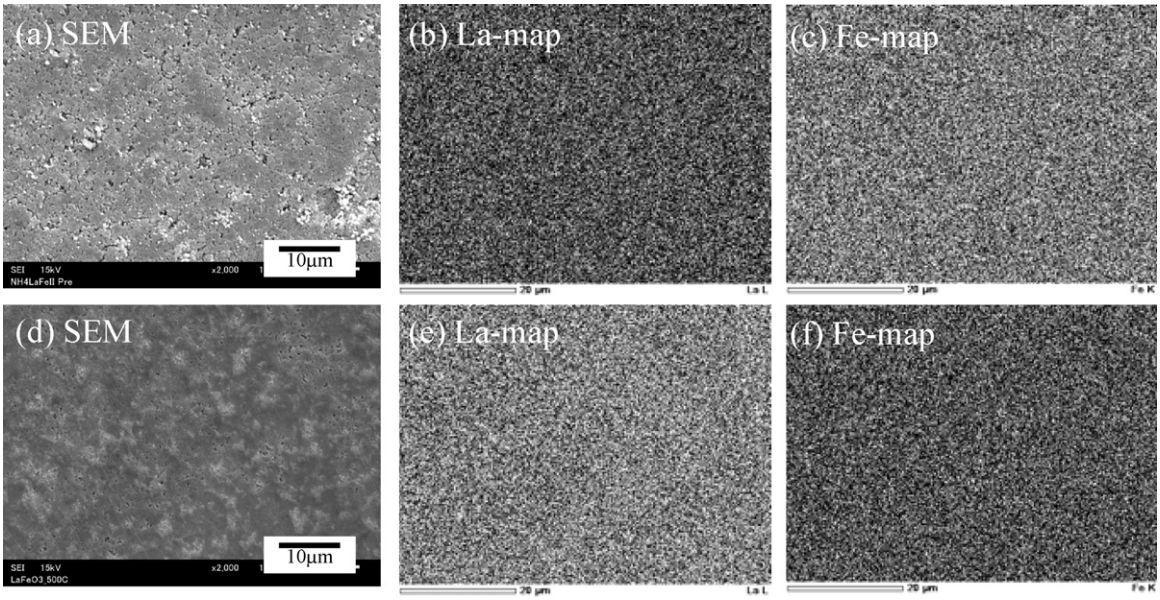

Fig. 9. SEM-EDX results of (a)–(c) the $(NH_4)La[Fe^{II}(CN)_6]\cdot nH_2O$ complex and (d)–(f) its decomposition product at 500 °C.

performed on the same surface observed by SEM (Fig. 9(a) and (d)). The elemental distribution of La and Fe was highly homogeneous for the complex and the decomposed sample.

4. Conclusion

New heteronuclear $(NH_4)RE^{III}[Fe^{II}(CN)_6]\cdot nH_2O$ complexes (RE = La, Ce, Pr, Nd, Sm, Gd, Dy, Y, Er, Lu) were synthesized, and their hydration number and crystal structure were estimated to be $n = 4$ and a hexagonal unit cell (space group: $P6_3/m$). Their thermal decomposition products were investigated, and the single phase of the perovskite-type materials was directly obtained by the decomposition of the heteronuclear complexes for RE = La, Pr, Nd, Sm, and Gd. The elemental distribution of RE and Fe was very homogeneous in these materials.

References

[1] J.G. McCarty, H. Wise, Perovskite catalysts for methane combustion, Catal. Today 8 (1990) 231–248.

[2] C. Tealdi, M.S. Islam, C.A.J. Fisher, L. Malavasi, G. Flor, Defect and transport properties of the $NdCoO_3$ catalyst and sensor material, Prog. Solid State Chem. 35 (2007) 491–499.

[3] A. Kaddouri, P. Gelin, N. Dupont, Methane catalytic combustion over La–Ce–Mn–O-perovskite prepared using dielectric heating, Catal. Commun. 10 (2009) 1085–1089.

[4] M. Asamoto, N. Harada, Y. Iwamoto, H. Yamamura, Y. Sadaoka, H. Yahiro, Catalytic activity of multi-metallic perovskite-type oxide prepared by the thermal decomposition of heteronuclear cyano complex, $Sm[Fe_xCo_{1-x}(CN)_6]\cdot nH_2O$, Top. Catal. 52 (2009) 823–827.

[5] Y. Wen, C. Zhang, H. He, Y. Yu, Y. Teraoka, Catalytic oxidation of nitrogen monoxide over $La_{1-x}Ce_xCoO_3$ perovskites, Catal. Today 126 (2007) 400–405.

[6] M. Mori, Y. Iwamoto, M. Asamoto, Y. Itagaki, H. Yahiro, Y. Sadaoka, S. Takase, Y. Shimizu, M. Yuasa, K. Shimanoe, H. Kusaba, Y. Teraoka, Effect of preparation routes on the catalytic activity over $SmFeO_3$ oxide, Catal. Today 139 (2008) 125–129.

[7] E. Arendt, A. Maione, A. Klisinska, O. Sanz, M. Montes, S. Suarez, J. Blanco, P. Ruiz, Structuration of $LaMnO_3$ perovskite catalysts on ceramic and metallic monoliths: physico-chemical characterisation and catalytic activity in methane combustion, Appl. Catal. A: Gen. 339 (2008) 1–14.

[8] N.Q. Minh, Ceramic fuel cells, J. Am. Ceram. Soc. 76 (1993) 563–588.

[9] F. L-Joud, G. Gauthier, J. Mougin, Current status of proton-conducting solid oxide fuel cells development, J. Appl. Electrochem. 39 (2009) 535–543.

[10] E.V. Tsipis, V.V. Kharton, Electrode materials and reaction mechanisms in solid oxide fuel cells: a brief review: I. Electrochemical behavior vs. materials science aspects, J. Solid State Electrochem. 12 (2008) 1367–1391.

[11] H. Aono, M. Sato, E. Traversa, M. Sakamoto, Y. Sadaoka, Design of ceramic materials for chemical sensors: effect of $SmFeO_3$ processing on its surface and electrical properties, J. Am. Ceram. Soc. 84 (2) (2001) 341–347.

[12] H. Aono, E. Traversa, M. Sakamoto, Y. Sadaoka, Crystallographic characterization and NO_2 gas sensing property of $LnFeO_3$ prepared by thermal decomposition of Ln–Fe hexacyanocomplexes, $Ln[Fe(CN)_6]\cdot nH_2O$, Ln = La, Nd, Sm, Gd, and Dy, Sens. Actuators B 94 (9) (2003) 132–139.

[13] Y. Hosoya, Y. Itagaki, H. Aono, Y. Sadaoka, Ozone detection in air using $SmFeO_3$ gas sensor, Sens. Actuators B 108 (2005) 198–201.

[14] Y. Itagaki, M. Mori, Y. Hosoya, H. Aono, Y. Sadaoka, O_3 and NO_2 sensing properties of $SmFe_{1-x}Co_xO_3$ perovskite oxides, Sens. Actuators B 122 (2007) 315–320.

[15] G.N. Chaudhari, S.V. Jagtap, N.N. Gedam, M.J. Pawar, V.S. Sangawar, Sol–gel synthesized semiconducting $LaCo_{0.8}Fe_{0.2}O_3$-based powder for thick film NH_3 gas sensor, Talanta 78 (2009) 1136–1140.

[16] K. Watanabe, M. Yuasa, T. Kida, K. Shimanoe, Y. Teraoka, N. Yamazoe, Oxygen permeation of a dense/porous asymmetric membrane using $La_{0.6}Ca_{0.4}CoO_{3-\delta}$-$BaFe_{0.975}Zr_{0.025}O_{3-\delta}$system, Chem. Lett. 38 (2009) 94–95.

[17] H. Michishita, Y. Misumi, D. Haruta, T. Masaki, N. Yamamoto, H. Matsumoto, T. Ishihara, Cathodic performance of $La_{0.6}Sr_{0.4}CoO_3$ perovskite oxide for platinum-free alkaline water electrolysis cell, J. Electrochem. Soc. 155 (2008) B969–B971.

[18] P.K. Gallagher, A simple technique for the preparation of R.E. FeO_3 and R.E. CoO_3, Mater. Res. Bull. 3 (1968) 225–232.

[19] Y. Sadaoka, H. Aono, E. Traversa, M. Sakamoto, Thermal evolution of nanosized $LaFeO_3$ powders from a heteronuclear complex, $La[Fe(CN)_6]\cdot nH_2O$, J. Alloys Compd. 278 (1998) 135–141.

[20] Y. Sadaoka, K. Watanabe, Y. Sakai, M. Sakamoto, Preparation of perovskite-type oxides by thermal decomposition of heteronuclear complexes, $\{Ln[Fe(CN)_6]\cdot nH_2O\}_x$, (Ln = La ∼ Ho), J. Alloys Compd. 224 (1995) 194–198.

[21] Y. Sadaoka, K. Watanabe, Y. Sakai, M. Sakamoto, Thermal decomposition behavior of heteronuclear complexes, $Ln[Co(CN)_6]\cdot nH_2O$, (Ln = La–Yb), J. Ceram. Soc. Jpn. 103 (1995) 519–522.

[22] Y. Sadaoka, E. Traversa, M. Sakamoto, Preparation and structural characterization of perovskite-type $La_xLn''_{1-x}CoO_3$ by the thermal decomposition of heteronuclear complexes, $La_xLn''_{1-x}[Co(CN)_6]\cdot nH_2O$ (Ln″ = Sm and Ho), J. Alloys Compd. 240 (1996) 51–59.

[23] Y. Sadaoka, E. Traversa, M. Sakamoto, Preparation and characterization of perovskite-type $Ln'Ln''_{1-x}CoO_3$ for electroceramic applications, J. Mater. Chem. 6 (1996) 1355–1360.

[24] M. Sakamoto, P. Nunziante, E. Traversa, S. Matsushima, M. Miwa, H. Aono, Y. Sadaoka, Preparation of perovskite-type oxides by the thermal decomposition of heteronuclear complexes, $Ln[Fe_xCo_{1-x}(CN)_6]\cdot 4H_2O$ (Ln = Pr ∼ Yb), J. Ceram. Soc. Jpn. 105 (1997) 963–969.

[25] E. Traversa, P. Nunziante, M. Sakamoto, Y. Sadaoka, R. Montanari, Synthesis and structural characterization of trimetallic perovskite-type oxides, $LaFe_xCo_{1-x}O_3$, by the thermal decomposition of cyano complexes, $La[Fe_xCo_{1-x}(CN_6)]\cdot nH_2O$, Mater. Res. Bull. 33 (1998) 673–681.

[26] F. Goubard, A. Tabuteau, On the lanthanide ferrocyanides $KLnFe(II)(CN)_6\cdot xH_2O$ (Ln = La-Lu): characterization and thermal evolution, J. Solid State Chem. 167 (2002) 34–40.

[27] F. Goubard, A. Tabuteau, Synthesis Spectroscopic Thermal and Structural Characterization of Complex Ferrocyanides $KLnFe^{(II)}(CN)_6\cdot 3.5H_2O$ (Ln = Gd–Ho), Struct. Chem. 14 (2003) 257–262.

[28] K. Sato, S. Itoh, K. Yamaguchi, M. Kurihara, M. Sakamoto, H. Aono, Y. Sadaoka, Preparation of perovskite-type oxide, $LaFeO_3$, by low-temperature decomposition of heteronuclear coordination polymer, $(NH_4)La[Fe(CN)_6]\cdot 4.5H_2O$, J. Ceram. Soc. Jpn. 118 (5) (2010) 384–386.

[29] D.F. Mullica, E.L. Sappenfield, H.O. Perkins, X-ray diffraction investigations and spectral analyses of monoclinic $SmKFe(CN)_6\cdot 3H_2O$, J. Solid State Chem. 78 (1989) 301–306.

[30] D.F. Mullica, E.L. Sappenfield, H.O. Perkins, Synthesis, spectroscopic, and structural investigation of ytterbium potassium hexacyanoferrate (II), $YbKFe(CN)_6\cdot 3.5H_2O$, J. Solid State Chem. 91 (1991) 98–104.

[31] W.O. Milligan, D.F. Mullica, H.O. Perkins, The structural analysis of $NdKFe(CN)_6\cdot 4H_2O$, Inorg. Chim. Acta 60 (1982) 35–38.

[32] G.W. Beall, D.F. Mullica, W.O. Milligan, The crystal structure of $LaKFe(CN)_6\cdot H_2O$, Acta Crystallogr. B 34 (1978) 1446–1449.

[33] D.F. Mullica, E.L. Sappenfield, H.O. Perkins, A structural investigation of praseodymium potassium hexacyanoferrate (II) tetrahydrate, $PrKFe(CN)_6\cdot 4H_2O$, J. Solid State Chem. 73 (1988) 65–70.

[34] R.D. Shannon, Revised effective ionic radii and systematic studies of interatomic distances in halides and chalcogenides, Acta Crystallogr. A 32 (1976) 751–767.

[35] F. Hulliger, M. Landolt, H. Vetsch, Rare-earth ferricyanides and chromicyanides $LnT(CN)_6\cdot nH_2O$, J. Solid State Chem. 18 (1976) 283–291.